Int J Adv Manuf Technol (2006) 29: 532–540
DOI 10.1007/s00170-005-2536-x

ORIGINAL ARTICLE

M. Kantha Babu · O.V. Krishnaiah Chetty

A study on the use of single mesh size abrasives in abrasive waterjet machining

Received: 23 July 2004 / Accepted: 31 December 2004 / Published online: 18 January 2006

Abstract This paper details the studies on the use of single mesh size garnet abrasives in abrasive waterjet machining for cutting aluminum. The influence of three different single mesh size abrasives, pressure, traverse rate, and abrasive flow rate; on depth of cut, top kerf width, bottom kerf width, kerf taper, and surface roughness are investigated. Experiments designed using standard L9 orthogonal array and the analysis of variance helped in the determination of highly significant, significant and weakly significant cutting parameters. Single mesh size abrasives are found to yield decreased surface roughness than multi mesh size abrasives. Based on these studies, response equations are developed to predict the target parameters. Using single mesh abrasives, a practitioner not only can cut faster but also achieve reduced surface roughness.

Keywords Abrasive waterjet machining · abrasive particle size distribution · orthogonal array · design of experiments · machining of aluminum · ANOVA analysis

1 Introduction

Abrasive waterjet machining (AWJM), with its wide-ranging applications, offers a wide variety of advantages [1]. It is very effective even in machining materials that are hard to machine [2]. It does not result in heat affected zone and involves minimum reactive forces [3, 4]. On the basis of jet generation, AWJs can generally be categorized as injection jets or suspension jets. An injection type AWJM system consists of a high-pressure intensifier, abrasive cutting head, positioning system, vibratory abrasive feeder, demineralization plant and a catcher tank. In this system the water jet emerges from a primary nozzle (typically 0.25 mm diameter) made of sapphire or diamond. Abrasives get mixed with the jet in a mixing chamber and moves through a focusing nozzle (typically 0.8 mm diameter) made of tungsten carbide with a velocity of 700–900 m/s [4]. Injection jets are currently being used in technically developed countries as shop floor facilities.

The intensity and the efficiency of the cutting process depend on several AWJM process parameters [4, 5]. They are classified as hydraulic, mixing/nozzle, cutting, and abrasive parameters. Depth of cut, surface roughness, volume removal rate, and kerf geometry – top kerf width, bottom kerf width and kerf taper are often used as target parameters. Hydraulic parameters consist of jet pressure (P) and the orifice diameter. Focusing tube length and tube diameter are the mixing/focusing nozzle parameters. Cutting parameters are traverse rate (TR), stand off distance, angle of impact, and number of passes. Abrasive parameters include the type of abrasive material, particle size, shape, particle size distribution (PSD), abrasive flow rate (AFR), recycling capacity, and the hardness of abrasives. Among these parameters, certain abrasive parameters such as abrasive particle size and shape of the abrasives and their distribution influence the target parameters [6–12].

Abrasive particles disintegrate during the acceleration and focusing process and also during cutting [8–12]. During the cutting process, breakdown of the abrasive particles occurs in two stages; 1) Particle/particle, particle/waterjet and particle/wall collisions in the mixing chamber/focusing tube assembly, and 2) Particle/particle and particle target collisions [8]. These interactions indicate that the particle size, shape as well as particle size distribution of abrasives before passing through the nozzle, after the nozzle exit, and after cutting differ widely from each other [8, 11, 12]. The changes in size, shape and PSD are based on the other process parameters as well as the target materials. Literature indicates that limited attempts are made to study the influence of PSD in machining. For the first time Momber and Kovacevic [7] studied the influence of two different particle size distribution parameters; size modulus of 150 microns to 400 microns and a distribution modulus 1 to 4, in aluminum machining. The distribution parameters used by them are derived from a Rosin-Rammler-Sperling grain size distribution The influence of these parameters on the depth of cut is not significant

M. Kantha Babu · O.V. Krishnaiah Chetty (✉)
Manufacturing Engineering Section,
Department of Mechanical Engineering,
Indian Institute of Technology Madras,
Chennai 600 036, India
E-mail: ovk@iitm.ac.in

in the selected parameter range, where as surface roughness in the smooth cutting zone is sensitive to changes in both of the particle size distribution parameters [7]. Kantha babu and Krishnaiah chetty [10, 11] also studied and reported the influence of particle size distribution on AWJM.

Cost of abrasives contributes substantially to the production cost. Industries prefer garnet abrasives (one of the popular abrasives) drawn from established sources [4, 13, 14]. Indian industries are focusing attention on the possible benefits of using AWJM in their production systems. Abrasives, if locally available may prove economical. Industries can be encouraged to use this efficient technology if cost reductions are demonstrated. This will provide them a competitive edge for manufacturing. This work therefore aims at the use of the locally available garnet abrasives obtained from southern part of India and study the influence of single mesh size abrasives. Preliminary work done with multi-mesh size particles of these local abrasives is reported [10, 11, 15–18]. Though single mesh size abrasives did not yield better results than multi-mesh size abrasives, there could be a bias on the single mesh size chosen [10, 11]. Hence this paper attempts to vary single mesh size abrasives and investigate. This is also an element of the strategy to harness the power of AWJM to help precision manufacturing.

The target parameters considered are depth of cut (d), top kerf width (kw_t), bottom kerf width (kw_b), kerf taper (k_t): defined as ratio of top kerf width to bottom kerf width, surface roughness (R_a) (refer Figs. 1 and 2). The fragmentation of abrasives during various stages are studied using American Foundrymen's Society (AFS) grain fineness number. The AFS grain fineness number is defined as the sum of product of weight of abrasive particles retained in each sieve in percentage and previous sieve mesh number, divided by the total percentage of abrasives retained in the set of sieves and the pan. This paper analyses the performance of garnet abrasive with three different single mesh size abrasives along with other process parameters and reports the findings achieved through standard L9 orthogonal array

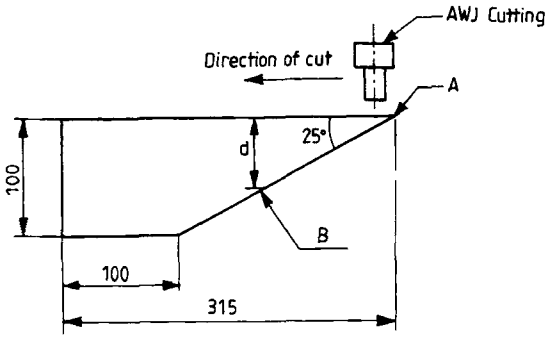

Fig. 1. Schematic of workpiece

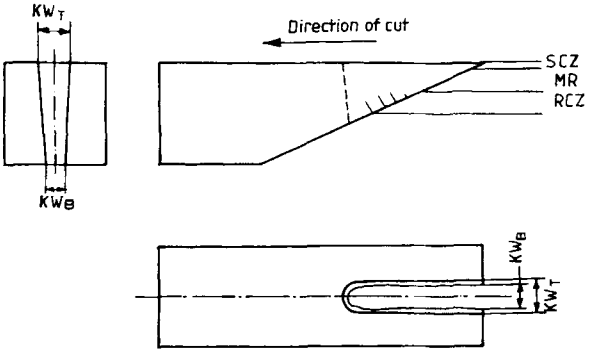

Fig. 2. Schematic view of a cut surface

(OA) experimentation. The response equations [19] are also established to predict the target parameters.

2 Experimental setup and procedure

The details of an injection type abrasive waterjet machine (Fig. 3) along with other equipment used for experimentation are shown

Fig. 3. Abrasive waterjet machining facility

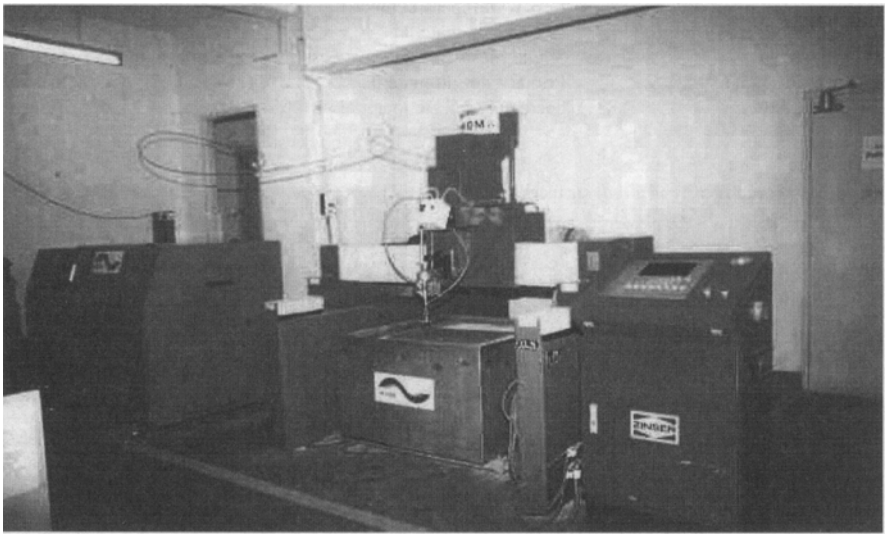

in Table 1. The constant process parameters are shown in Table 2. The variable process parameters shown in Table 3, describe the three levels of parameters namely pressure (P), traverse rate (TR), and abrasive flow rate (AFR), and abrasive samples (AS). The abrasive samples used are particles retained on three different single sieves designated as SC1, SC2, and SC3 (SC1: 0.315–0.355 mm/#52 mesh size, SC2: 0.250–0.315 mm/#60 mesh size, and SC3: 0.180–0.200 mm/#80 mesh size).

A trapezoidal work piece has been cut and the depth of machining d, ($d = AB \sin 25°$) is determined as shown in Fig. 1 Each combination of parameters can achieve certain depth of cut, indicated to the operator by splashing of jet. The length of cut over each test run is therefore a variable that depends on the chosen process parameters. The top and bottom kerf widths are measured at three locations on the cut length; at the start of cut, middle, and end of cut and then averaged (Fig. 2). The kerf taper is computed. In an AWJM cut surface, the upper section consists of a smooth cutting zone (SCZ) characterized as roughness, while the lower section consists of rough cutting zone (RCZ) characterized as waviness [20]. Kovacevic [19] has measured the surface roughness at three levels across the thickness of the cut at 1.58 mm, 3.17 mm, and 4.76 mm. In this experimentation work, upper (2 mm from the top surface), middle and lower (two third height from the top surface) sections of the machined surface of aluminum material are selected for surface roughness measurement and compared. The photographs of a typical cut surfaces are shown in Fig. 4. The measurements of surface roughness (R_a) are made in the direction of jet traverse. Abrasive particles have been collected at the exit of the focusing nozzle, and also after cutting the material and AFS grain fineness number are determined. Collection is done through a special catcher, consisting of a cylindrical drum with a screening cloth. The collected abrasives are cleaned (aluminum debris is dissolved by adding 20% NaOH solution), dried and sieved.

Table 2. Constant process parameters

Abrasive material	Garnet
Abrasive particle shape	Angular (random)
Primary Nozzle diameter	0.25 mm
Secondary Nozzle diameter	0.8 mm
Secondary Nozzle Length	70 mm
Stand off distance	3 mm
Jet impact angle	90°

Table 3. Variable process parameter

S. No	Variable parameter	Low 1	Medium 2	High 3
1	Pressure [MPa]	150	225	300
2	Traverse rate [mm/min]	50	125	200
3	Abrasive flow rate [g/s]	0.5	1.0	1.5
4	Abrasive sample code	SC1	SC2	SC3
	[mm]	(0.315–0.355)	(0.250–0.315)	(0.180–0.200)
	Single mesh size	#52	#60	#80
	AFS number	44	52	72

Table 1. Details of the equipments

Item	Description
Abrasive Waterjet Machining System	Pressure intensifier, Injection type nozzle
Power	22 kW, 50 Hz
Max. Discharge pressure	360 MPa
Abrasive feeding system	Vibratory conveyor with heating facility
CNC work table	Two-axis control (X=1000,Y=1000)
British Standard Sieves, Mesh number	30,36,44,52,60,72,80,100,120,
Surface Finish measuring equipment	Perthometer, Cut off length: 0.8 mm, traverse length: 4.8 mm
Kerf width measurement	Optical microscope, 0.5 microns accuracy
Work piece material	Aluminium 6063 T6
Single mesh size abrasives used for experimentation	#52, #60, #80,
Primary nozzle material	Sapphire
Secondary nozzle material	Tungsten Carbide

Fig. 4. Photographs of typical cut surfaces

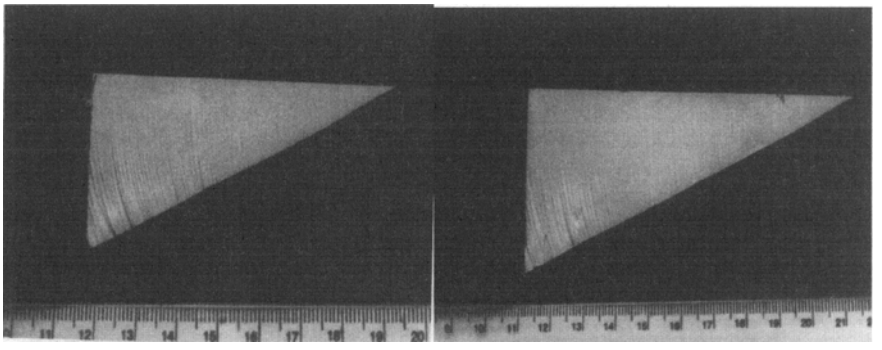

Table 4. L9 Orthogonal Array

Ex. No	Pressure (P) A	Traverse rate (TR) B	Abrasive flow rate (AFR) C	Abrasive sample code (AS) D
1	1	1	1	1
2	1	2	2	2
3	1	3	3	3
4	2	1	2	3
5	2	2	3	1
6	2	3	1	2
7	3	1	3	2
8	3	2	1	3
9	3	3	2	1

Table 5. Allocation of parameters

Ex. No	Pressure (P) [MPa] A	Traverse rate (TR) [mm/min] B	Abrasive flow rate (AFR) [g/s] C	Abrasive sample code (AS) D
1	150	50	0.5	SC1
2	150	125	1	SC2
3	150	200	1.5	SC3
4	225	50	1	SC3
5	225	125	1.5	SC1
6	225	200	0.5	SC2
7	300	50	1.5	SC2
8	300	125	0.5	SC3
9	300	200	1	SC1

L9 orthogonal array (OA) has been used to minimize experimentation [16, 19, 22–26]. The details of the standard L9 OA and allocation of parameters are shown in Tables 4 and 5. Statistically designed experiments perform more efficiently than traditional methods as they consider multiple factors simultaneously and can detect important interactions. The results are analyzed through ANOVA technique. ANOVA is a computational technique that helps to estimate the relative contributions of each control factor. ANOVA provides insight into the main effects, interaction effects of factors and as well as noise. This will be useful in decision making to determine the control factors for further expenditure of resources. Randomized experimentation without replication has been done.

3 Results and discussion

Analyses considering depth of cut, top kerf width, bottom kerf width, kerf taper and surface roughness are presented hereunder. The experimental results are shown in Table 6.

3.1 Depth of cut

Detailed ANOVA analysis in Table 7 concerning depth of cut indicates that only TR is found to be weakly significant at 10% level. Its linear effect is significant at 10% level, while quadratic effect is not significant. The mean response in Fig. 5 indicates that lower traverse rate (TR1) results in maximum depth of cut. Lower traverse rate implies prolonged exposure time and hence increased depth of machining. Hence the behaviour of single mesh size abrasives is in line with multi-mesh size abrasives [4, 5, 9–11, 21, 27, 28]. The response equation for depth of cut of individual main parameters, Y_{DOC} is:

$$Y_{DOC} = 18.43 + 0.113(P - 225) - 0.150(TR - 125) + 1.70 \times 10^{-3}(TR - 125)^2 + 12.66(AFR - 1) + 50(AS - 0.250) \quad (1)$$

3.2 Kerf width

Kerf width (average of three measurements) is measured by using optical microscope at the top and bottom surfaces of the cut. The kerf taper is computed in each case. The results of kerf geometry are shown in Table 6. It is observed that the bottom kerf width is smaller than top kerf width, resulting in a convergent cut. These findings concerning single mesh size abrasives

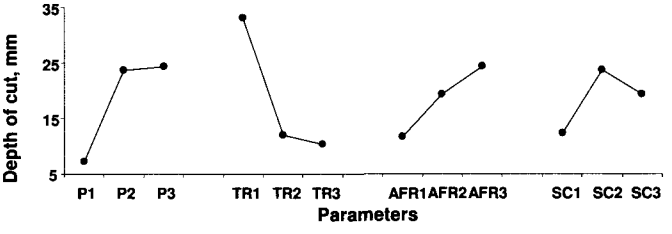

Fig. 5. Mean responses – parameters vs depth of cut, mm

Table 6. Experimental results

Ex. No	Depth of cut [mm]	Kerf Width [mm] Top surface average	Bottom surface average	Kerf taper	Surface Roughness, [R_a] Upper	Middle	Lower	AFS No. at nozzle exit	AFS No. after cutting
1	9	1.01	0.74	1.36	8.1	9.6	11.0	77	98
2	7	1.07	0.86	1.25	5.5	6.0	6.6	78	92
3	6	0.94	0.88	1.06	7.4	8.1	9.1	96	109
4	40	0.95	0.69	1.39	6.7	6.9	8.1	97	124
5	17	0.94	0.78	1.20	6.5	5.5	7.6	84	107
6	14	1.05	0.90	1.16	7.1	8.1	11.3	81	99
7	50	1.12	0.97	1.15	7.5	7.2	8.5	98	112
8	12	1.15	0.68	1.69	5.7	6.6	10.9	92	96
9	11	1.04	0.73	1.43	5.1	5.3	6.6	95	110

Table 7. Detailed ANOVA analysis on depth of cut

Source	Pool	DF	S	V	F*	S′	ρ, %	Remarks
P		2	556.22	278.11	2.53	336.00	17.19	Ns
TR		2	957.56	478.78	4.35	737.34	37.73	*
TR_L		1	770.89	770.89	7.00	660.78	33.81	*
TR_Q		1	186.67	186.67	1.69	75.56	3.87	Ns
AFR	Y	2	244.22	122.11	–	–	–	Ns
AS	Y	2	196.22	98.11	–	–	–	Ns
(e)		4	440.44	110.11	–	880.89	45.08	–
Total		8	1954.22	244.28	–	–	–	–

* F' 0.10, 2, 4 = 4.32, F' 0.05, 2, 4 = 6.94, F' 0.01, 2, 4 = 18.0
* F' 0.10, 1, 4 = 4.54, F' 0.05, 1, 2 = 7.71, F' 0.01, 1, 2 = 16.3

Nomenclature

Y	Pooled	DF	Degree of freedom
*	Weekly significant at 10% level.	S	Sum of squares
**	Significant at 5% level.	V	Variance
***	Highly significant at 1% level.	F	F-ratio
Ns	Not Significant	S′	Pure sum of square
L	Linear effect	ρ,%	Percentage contribution
Q	Quadratic effect		

are found to be in line with the results obtained with multi-mesh sizes of garnet abrasives [4, 5, 9–11, 21, 27, 28].

3.2.1 Top kerf width

Detailed ANOVA analysis in Table 8 concerning top kerf width indicates that only pressure is found to be weakly significant at 10% level. The linear effect of pressure is weakly significant at 10% level, while its quadratic effect is not significant. From the mean response Fig. 6, it is observed that medium pressure (P2) results in minimum kerf width. Minimum kerf width is advantageous in machining because of minimum material is lost. The response equation for top kerf width of individual main and significant parameters, Y_{KWT} is:

$$Y_{KWT} = 0.98 + 6.4 \times 10^{-4}(P - 225) + 1.33 \times 10^{-5}(P - 225)^2 - 1.13 \times 10^{-4}(TR - 125) - 0.07(AFR - 1) + 0.114(AS - 0.251) \quad (2)$$

3.2.2 Bottom kerf width

Detailed ANOVA analysis in Table 9 concerning bottom kerf width indicates that abrasive flow rate is weakly significant and abrasive samples is significant at 5% levels. The linear effect of AFR is weakly significant at 10% level and its quadratic effect is not significant. The linear effect of AS is not significant, while its quadratic effect is significant at 5% level. This is in deviation from the multi-mesh size abrasives behaviour [11].

The mean response in Fig. 7 indicates that at medium abrasive flow rate (AFR2) and abrasive samples both SC1 and SC3 result in minimum bottom kerf width. This may be construed as medium abrasive flow rate resulting in optimum abrasive flow rate, while machining with single abrasive particles. Minimum bottom kerf width may result when the energy available is reduced or jet deflections/instability is reduced. The complex combinations of AFR2, SC1, and SC3 seem to reduce jet deflections/instability. The response equation for bottom kerf width of individual main and significant parameters, Y_{KWB} is:

$$Y_{KWB} = 0.859 - 2.27 \times 10^{-4}(P - 225) + 2.47 \times 10^{-4}(TR - 125) + 0.144(AFR - 1) + 0.264(AFR - 1)^2 + 30.61(AS - 0.250)^2 \quad (3)$$

Table 8. Detailed ANOVA analysis on top kerf width

Source	Pool	DF	S	V	F*	S′	ρ, %	Remarks
P		2	0.026	0.013	9.337	0.023	46.939	*
P_L		1	0.014	0.014	10.815	0.013	26.531	*
P_Q		1	0.011	0.011	8.446	0.010	20.408	Ns
TR	Y	2	0.003	0.001	1.000	0.001	2.041	Ns
AFR		2	0.008	0.004	2.888	0.005	10.204	Ns
AS		2	0.012	0.006	4.410	0.009	18.367	Ns
(e)		2	0.003	0.001	–	0.011	22.449	–
Total		8	0.049	0.006	–	–	–	–

* F' 0.10, 2, 2 = 9.0, F' 0.05, 2, 2 = 19.0, F' 0.01, 2, 2 = 99.0
* F' 0.10, 1, 2 = 8.53, F' 0.05, 1, 2 = 18.5, F' 0.01, 1, 2 = 93.5

Table 9. Detailed ANOVA analysis on bottom kerf width

Source	Pool	DF	S	V	F*	S′	ρ, %	Remarks
P	Y	2	0.003	0.001	1.000	0.001	1.163	Ns
TR		2	0.006	0.003	2.547	0.004	4.651	Ns
AFR		2	0.025	0.013	9.859	0.023	26.744	*
AFR_L		1	0.016	0.016	12.202	0.015	16.984	*
AFR_Q		1	0.010	0.010	7.445	0.009	9.909	Ns
AS		2	0.052	0.026	20.467	0.050	58.140	**
AS_L		1	0.000	0.000	0.001	0.001	1.161	Ns
AS_Q		1	0.052	0.052	40.785	0.051	59.494	**
(e)		2	0.003	0.001	–	0.010	11.628	–
Total		8	0.086	0.011	–	–	–	–

* F' 0.10, 2, 2 = 9.0, F' 0.05, 2, 2 = 19.0, F' 0.01, 2, 2 = 99.0
* F' 0.10, 1, 2 = 8.53, F' 0.05, 1, 2 = 18.5, F' 0.01, 1, 2 = 93.5

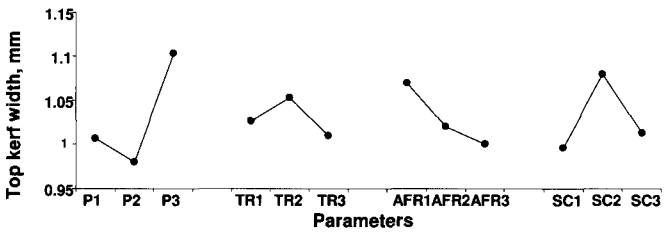

Fig. 6. Mean responses – parameters vs top kerf width, mm

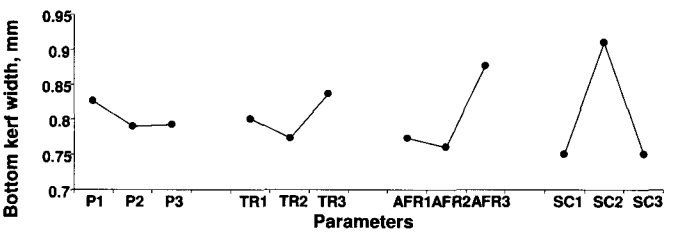

Fig. 7. Mean responses – parameters vs bottom kerf width, mm

3.2.3 Kerf taper

ANOVA analysis in Table 10 indicated that no parameter influences kerf taper even at 10% level. This behaviour is similar to that of multi-mesh size abrasives reported [11]. The variation observed in the present case may be explained by the observations of Hashish [20]; that the cutting could be irregular because of non-uniformity of fragmented abrasive distribution in the jet, and side deflection of cutting stream resulting in jet instability, leading to erosion that may mask the basic geometry. The mean response is given in Fig. 8 and the response equation for kerf taper of individual main parameters, Y_{KT} is:

$$Y_{KT} = 1.299 + 1.33 \times 10^{-3}(P - 225) - 1.77 \times 10^{-3}(TR - 125) - 0.083(AFR - 1) + 18.558(AS - 0.251) \quad (4)$$

3.3 Surface roughness

Surface roughness (R_a) measurements are made using perthometer at three locations of the cut surface. a) upper section b) middle section, and c) lower section. The results are shown in Table 6. Detailed ANOVA analysis for the surface roughness is shown in Tables 11, 12, and 13 and the mean analysis is shown in Figs. 9, 10 and 11.

3.3.1 Upper section

Detailed ANOVA analysis in Table 11 concerning surface roughness at the upper section of the material indicates that pressure, traverse rate, and abrasive flow rate are significant at 5% level. The significance of linear and quadratic effects is also shown in this table. This is in deviation from the findings of [10, 11, 27]. This may be attributed to the wide range of abrasive particles used in their experimentation. Therefore preciously controlled abrasive samples along with other parameters could influence the surface roughness at the upper section also. The mean response in Fig. 9, indicates that highest pressure (P3), medium traverse rate (TR2), and medium abrasive flow rate (AFR2) result in de-

Table 10. Detailed ANOVA analysis on kerf taper

Source	Pool	DF	S	V	F*	S′	ρ, %	Remarks
P		2	0.071	0.035	1.808	0.032	10.93	Ns
TR	Y	2	0.039	0.020	1.000	0.001	0.345	Ns
AFR		2	0.120	0.060	3.072	0.081	28.05	Ns
AS		2	0.059	0.030	1.507	0.020	6.86	Ns
(e)		2	0.039	0.020	–	0.157	54.15	–
Total		8	0.290	0.036	–	–	–	–

* F' 0.10, 2, 2 = 9.0, F' 0.05, 2, 2 = 19.0, F' 0.01, 2, 2 = 99.0

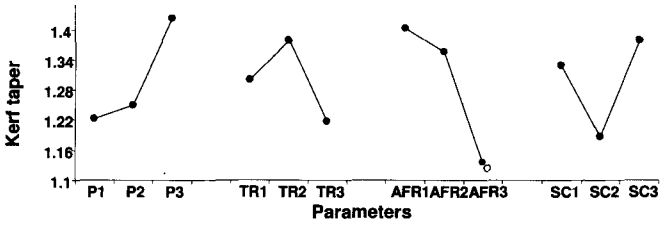

Fig. 8. Mean responses – parameters vs kerf taper

Table 11. Detailed ANOVA analysis on surface roughness in the upper section

Source	Pool	DF	S	V	F*	S′	ρ, %	Remarks
P		2	1.309	0.654	45.308	1.280	15.54	**
P_L		1	1.215	1.215	86.785	1.200	14.57	**
P_Q		1	0.094	0.094	6.714	0.080	0.97	Ns
TR		2	3.562	1.781	123.308	3.533	42.90	**
TR_L		1	1.215	1.215	86.785	1.201	14.58	**
TR_Q		1	2.347	2.347	167.64	2.332	28.31	***
AFR		2	3.336	1.668	115.462	3.308	40.15	**
AFR_L		1	0.039	0.039	2.785	0.025	0.30	Ns
AFR_Q		1	3.321	3.321	237.214	3.307	40.15	***
AS	Y	2	0.029	0.014	1.000	0.986	11.97	Ns
(e)		2	0.029	0.014	–	0.001	1.40	–
Total		8	8.236	1.029	–	–	–	–

* F' 0.10, 2, 2 = 9.0, F' 0.05, 2, 2 = 19.0, F' 0.01, 2, 2 = 99.0
* F' 0.10, 1, 2 = 8.53, F' 0.05, 1, 2 = 18.5, F' 0.01, 1, 2 = 93.5

Table 12. Detailed ANOVA analysis on surface roughness in the middle section

Source	Pool	DF	S	V	F*	S′	ρ, %	Remarks
P		2	3.707	1.853	14.256	3.447	22.21	*
P_L		1	3.510	3.510	27.000	3.380	21.77	**
P_Q		1	0.197	0.197	1.153	0.067	0.43	Ns
TR		2	5.307	2.653	20.410	5.047	32.52	**
TR_L		1	0.799	0.799	6.146	0.669	4.31	Ns
TR_Q		1	4.508	4.508	34.676	4.378	28.20	**
AFR		2	6.247	3.123	24.026	5.987	38.57	**
AFR_L		1	2.050	2.050	15.769	1.920	12.37	*
AFR_Q		1	4.197	4.197	32.284	4.067	26.20	**
AS	Y	2	0.260	0.130	1.000	0.000	–	Ns
(e)		2	0.260	0.130	–	1.040	6.70	–
Total		8	15.520	1.940	–	–	–	–

* F' 0.10, 2, 2 = 9.00, F' 0.05, 2, 2 = 19.0, F' 0.01, 2, 2 = 99.0
* F' 0.10, 1, 2 = 8.53, F' 0.05, 1, 2 = 18.5, F' 0.01, 1, 2 = 93.5

Table 13. Detailed ANOVA analysis on surface roughness in the lower section

Source	Pool	DF	S	V	F*	S′	ρ, %	Remarks
P	Y	2	0.176	0.088	1.000	1.000	3.66	Ns
TR		2	1.136	0.568	6.468	0.960	3.52	Ns
AFR		2	24.536	12.268	139.759	24.360	89.35	***
AFR_L		1	10.690	10.690	121.47	10.602	38.88	***
AFR_Q		1	13.846	13.846	157.34	13.758	50.46	***
AS		2	1.416	0.708	8.063	1.240	4.55	Ns
(e)		2	0.176	0.088	–	0.702	2.58	–
Total		8	27.262	3.408	–	–	–	–

* F' 0.10, 2, 2 = 9.00, F' 0.05, 2, 2 = 19.0, F' 0.01, 2, 2 = 99.0
* F' 0.10, 1, 2 = 8.53, F' 0.05, 1, 2 = 18.5, F' 0.01, 1, 2 = 93.5

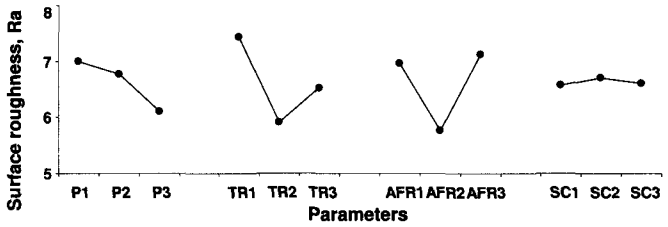

Fig. 9. Mean responses – parameters vs surface roughness, R_a at upper section

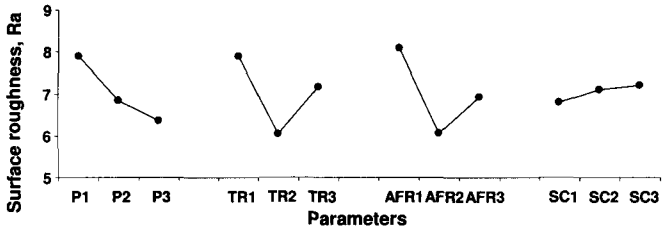

Fig. 10. Mean responses – parameters vs surface roughness, R_a at middle section

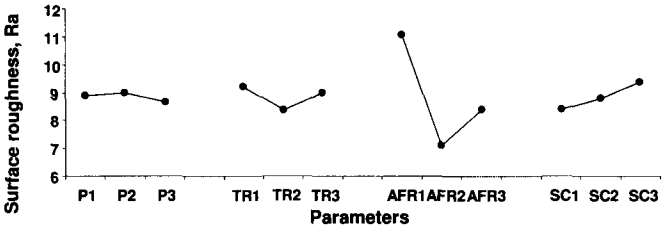

Fig. 11. Mean responses – parameters vs surface roughness, R_a at lower section

creased surface roughness while using single mesh size abrasive. The response equation for the upper section of individual main and significant parameters, Y_{SRU} is:

$$Y_{SRU} = 6.40 - 6 \times 10^{-3}(P-225) + 4.41 \times 10^{-5}(P-225)^2 - 6 \times 10^{-3}(TR-125) + 1.92 \times 10^{-4}(TR-125)^2 + 0.16(AFR-1) - 0.323(AFR-1)^2 - 0.214(AS-0.250) \quad (5)$$

3.3.2 Middle section

Detailed ANOVA analysis in Table 12 concerning surface roughness at the middle section of the work material indicates that pressure is significant at 10% level, while traverse rate and abrasive flow rate are significant at 5% level. The significance of linear and quadratic effects is also shown in Table 12. The significant factors herein are similar to that of the upper section. From the mean response in Fig. 10, it is found that highest pressure (P3), medium traverse rate (TR2), and medium abrasive flow rate (AFR2) resulted in decreased surface roughness.

Higher pressure normally increases the fragmentation of abrasives because of increased kinetic energy [28]. Analysis of AFS number with multi-mesh size abrasives has shown this trend [11]. However while machining with single mesh size abrasives, though AFS grain finesses number (Figs. 12 and 13) changed, it is found to be insignificant (Tables 6, 14, 15). Hence single mesh abrasives behaviour deviated from that of multi-mesh size abrasives.

In the case of traverse rate, medium traverse rate (TR2) resulted in decreased surface roughness, however traverse rate did not significantly influence the fragmentation of single mesh size abrasive particles (Tables 14, 15). Similar trend was reported with multi-mesh size abrasives [11], However lower traverse rate

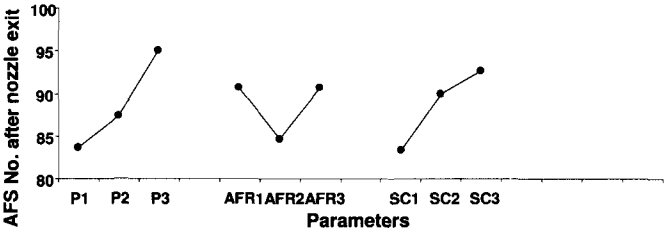

Fig. 12. Mean responses – parameters vs AFS no. after nozzle exit

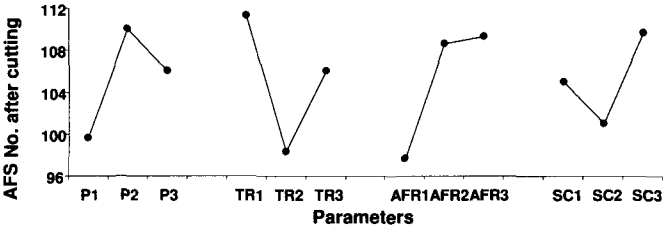

Fig. 13. Mean responses – parameters vs AFS no. after cutting

Table 14. Detailed ANOVA analysis on AFS grain fineness number after nozzle exit

Source	Pool	DF	S	V	F*	S′	ρ, %	Remarks
P		2	200.667	100.333	2.787	128.667	21.73	Ns
AFR		2	72.000	36.000	–	–	–	Ns
AS		2	138.667	69.333	1.926	66.667	11.26	Ns
E		2	180.667	90.333	2.509	108.667	18.36	Ns
(e)		2	72.000	36.000		288.000	48.65	–
Total		8	592.000	74.000	–	–	–	–

* F' 0.10, 2, 2 = 9.00, F' 0.05, 2, 2 = 19.0, F' 0.01, 2, 2 = 99.0

Table 15. Detailed ANOVA analysis on AFS grain fineness number after cutting

Source	Pool	DF	S	V	F*	S′	ρ, %	Remarks
P		2	162.889	81.444	1.443	50.000	6.33	Ns
TR		2	256.222	128.111	2.270	143.333	18.15	Ns
AFR		2	257.556	128.778	2.281	144.667	18.32	Ns
AS	Y	2	112.889	56.444	–	–	–	Ns
(e)		2	112.889	56.444	–	451.556	57.19	–
Total		8	789.556	98.694	–		–	–

* F' 0.10, 2, 2 = 9.00, F' 0.05, 2, 2 = 19.0, F' 0.01, 2, 2 = 99.0

(TR1) emerged as the best option for minimum surface roughness. This finding is significant; since the practical user can increase the traverse rate as well achieve better finish.

In the case of abrasive flow rate, the medium abrasive flow rate (AF2) results in minimum surface roughness, while it is insignificant with multi mesh size abrasives [11]. Hence single mesh size abrasive behaviour differs from multi-mesh size abrasive. The response equation for the middle section of individual main and significant parameters, Y_{SRM} is:

$$\begin{aligned} Y_{SRM} = {} & 3.187 - 0.01(P-225) + 5.38 \times 10^{-5}(P-225)^2 \\ & - 4.8 \times 10^{-3}(TR-125) + 2.67 \times 10^{-4}(TR-125)^2 \\ & - 1.17(AFR-1) + 5.77(AFR-1)^2 \\ & + 2.85(AS-0.250) \end{aligned} \quad (6)$$

3.3.3 Lower section

Detailed ANOVA analysis in Table 13 concerning surface roughness at the lower section of the work material indicates that only the abrasive flow rate is highly significant at 1% level. The significance of linear and quadratic effects is also shown in Table 13. The mean response in Fig. 11 indicates that medium abrasive flow rate (AFR2) results in decreased surface roughness. With single mesh size abrasives the abrasive flow rate is highly significant, while with multi-mesh size abrasive particles, pressure was found to be significant [11]. Hence single mesh size abrasive behaviour deviates from multi-mesh size abrasives. The response equation for the lower section of individual main parameters, Y_{SRU} is:

$$\begin{aligned} Y_{SRU} = {} & 1.826 - 1.53 \times 10^{-3}(P-225) \\ & - 1.33 \times 10^{-3}(TR-125) - 2.67(AFR-1) \\ & + 10.54(AFR-1)^2 - 6.92(AS-0.250) \end{aligned} \quad (7)$$

4 Conclusions

Abrasive waterjet machining is emerging as an effective machining technique at shop floor level. In this context, it is essential to optimize the process parameters. This paper discusses the abrasive waterjet machining of aluminum with the use of design of experiments L9 orthogonal array and the establishment of response equations. The influence of pressure, traverse rate, abrasive flow rate and specially formulated abrasive samples having three different single mesh size abrasives are analyzed. The target parameters namely depth of cut, top kerf width, bottom kerf width, and kerf taper, and surface roughness are studied. The results are summarized as follows:

1. Single mesh size abrasives behave similar to multi-mesh size abrasives in the achievable depth of cut.
2. Single mesh size abrasives deviates in its behavoiur from multi-mesh size abrasives considering top kerf width, bottom kerf width and kerf taper.
3. Considering surface roughness of machined surface, single mesh size deviates in its behaviour compared to multi-mesh size. The results of the surface roughness with single mesh size abrasives at the upper and middle section of the material are note worthy.
4. The response equations developed in this work will be useful to the manufacturing engineers to select suitable parameters of abrasives for a specific application of aluminum cutting.

The overall influence of single mesh size is that it provides a faster cutting (TR2) than while using multi-mesh size abrasives. This will help the practitioner to cut at a faster rate and also achieve reduced surface roughness. From a research point of view this helps to harness the power of AWJM towards precision manufacturing.

Acknowledgement The authors express sincere thanks to Science and Engineering Research Council of Department of Science & Technology, Government of India, for the financial support for the equipment. They also acknowledge the financial assistance for research interactions with German counterparts under the DST-DAAD project based personnel exchange program 1999.

References

1. Hashish M (1998) Waterjet advances in field and factory. Proceedings of 5th Pacific Rim International Conference on Waterjet Technology, New Delhi, India 231–246
2. Hashish M (1984) A modelling study of metal cutting with abrasive water jets. Transactions of ASME Journal of Engineering for Industry 106:88–100
3. Louis H (1998) Abrasive waterjets: A Review. Proceedings of 5th Pacific Rim International Conference on waterjet technology, New Delhi, India 321–329
4. Momber A, Kovacevic R (1988) Principles of abrasive waterjet machining. Springer –Verlag, London
5. Hashish M (1991) Optimisation factors in abrasive waterjet machining. Transactions of ASME Journal of Engineering for Industry 113:29–37
6. Momber A, Pfeiffer, Kovacevic R, Schunemann (1996) The Influence of abrasive grain size distribution parameters on the abrasive waterjet machining process. Proceedings of the 1996 24th NAMRI conference, Society of Manufacturing Engineers MR96(115):1–6
7. Momber A, Kovacevic R (2000) Particle size distribution influence in high speed erosion of aluminium. Particle Science and Technology 18:199–212
8. Labus T, Neusen K, Alberts D, Gores T (1991) Factors influencing the particle size distribution in an abrasive waterjet. Transactions of the ASME, Journal of Engineering for Industry 113:402–411
9. Krishnaiah Chetty OV, Ramesh Babu N (1999) Some investigations on abrasives in abrasives waterjet machining. Proceeding of 10th American waterjet conference, Waterjet Technology Association, USA: 419–430
10. Kantha Babu M, Krishnaiah Chetty OV (2001) Studies on the use of local abrasives in abrasive waterjet machining. Proceedings of 17th International conference on CAD/CAM, Robotics and Factories of Future, Durban, South Africa: 150–156
11. Kantha Babu M, Krishnaiah Chetty OV (2001) Abrasive waterjet machining of aluminium with local abrasives. Proceedings of 11th American WaterJet Conference, WaterJet Technology Association, Minneapolis, USA: 325–341
12. Guo N, Louis H, Meier G, Ohlsen J (1992) Recycling capacity of abrasives in Abrasive WaterJet cutting. Proceedings of 11th International conference on Jet Cutting Technology, Scotland 503–523
13. Hashish M (1989) A model for abrasive waterjet machining. Transactions of the ASME, Journal of Engineering Materials and Technology 111:154–162

14. Matsumoto K, Arasawa H, Yamaguchi S (1998) A study of the effect of abrasive material on cutting with abrasive waterjet. Proceedings of 9th International symposium of jet cutting technology, Sendai, Japan 255–269
15. Kantha Babu M, Krishnaiah Chetty OV (2002) Studies on recharging of abrasives in abrasive waterjet machining. International Journal of Advanced Manufacturing Technology, Springer-Verlag, London 19:697–703
16. Kantha Babu M, Krishnaiah Chetty OV (2003) A study on recycling of abrasives in abrasive waterjet machining. International Journal of Wear, Elsevier Science, Ireland 254:763–773
17. Kantha Babu M, Krishnaiah Chetty OV (2003) Studies on abrasive waterjet machining of black granite through design of experiment. International Journal of Experimental Techniques, September: 49–54
18. Kantha Babu M, Krishnaiah Chetty OV (2002) Abrasive waterjet machining of black Granite with garnet abrasives. Journal of the Institution of Engineers, Calcutta, India 83:7–14
19. Montgomery DC (1991) Design and Analysis of Experiments. John Wiley & Sons Inc, Singapore
20. Hashish M (1988) Visualisation of the abrasive-waterjet cutting process. Experimental Mechanics 28:159–168
21. Kovacevic R (1991) Surface texture in abrasive waterjet cutting. Journal of Manufacturing systems 10:32–40
22. Park SH (1996) Robost Design and Analysis for Quality Engineering, Chapman & Hall, London
23. Ross PJ (1996) Taguchi Techniques for Quality Engineering, Mcgraw-Hill Int. Editions, Singapore
24. William YF, Creveling CM (1995) Engineering methods for Robust Product design, Addison- Wesley Publishing Company, Massachusetts
25. Roslund J (1988) How to perform a Designed Experiments (DOE). International Journal of Experimental Techniques, April: 31–34
26. Rani RM, Seshan S (1988) Studies on abrasive jet machining through statistical design of Experiments. International Journal of Experimental Techniques, April: 28–30
27. Hashish M (1991) Characteristics of surfaces machined with abrasive waterjet. Transactions of the ASME Journal of Engineering Materials and Technology 113:354–362
28. Hashish M (1989) Pressure effects in abrasive waterjet (AWJ) machining. Transactions of ASME Journal of Engineering Materials and Technology 111:221–228